Supplementary Information

Bio-based Superaerophobic Hydrogels to Regulate Bubble Dynamics in Gas-Evolving Electrocatalysis

Sushmit Sen, Amrita Chatterjee, Pradip K. Maji*

Department of Polymer and Process Engineering, Indian Institute of Technology Roorkee, Saharanpur Campus, Saharanpur- 247001, India

*Corresponding Author: Pradip K. Maji (Email ID: pradip@pe.iitr.ac.in);

Contact no: +91-7895965010

Section S1:

Materials and Methods

Materials

Chitosan (derived from shrimp shells, molecular weight range of 3000-20000 Da[1], and degree of deacetylation ≥75%), glutaraldehyde solution (25 wt%), and acetic acid were obtained from TCI, India and used without further purification. Nickel foam (thickness ≈ 1.6 mm, porosity ≈ 95%) was purchased from Shilpa Enterprises. All aqueous solutions were prepared using deionized water.

Preparation of CS-GA Hydrogel

Chitosan (with a molecular weight of 3000-20000 Da and degree of deacetylation ≥75% was used to ensure sufficient chain mobility for conformal coating on Ni foam while maintaining a high density of protonatable amine groups for effective interfacial interaction and subsequent glutaraldehyde crosslinking) was dissolved in 1 wt.% acetic acid solution under magnetic stirring until a transparent solution was obtained. Different amounts of glutaraldehyde were then added dropwise to adjust the crosslinking density. The prepared solutions corresponded to 2.5, 5, and 10% GA relative to the chitosan content. The mixtures were stirred for 2 h at room temperature and allowed to form hydrogels.

Electrode Coating

Nickel foam substrates were cleaned via ultrasonication in deionized water for 15 min each and dried in a hot air oven. The cleaned foams were immersed in the prepared hydrogel precursor solutions, removed slowly, and dried at 40 °C. Samples were denoted as CS2.5GA, CS5GA, and CS10GA according to the GA content. Bare NF was used as a control.

Characterization

FTIR spectra were recorded on a PerkinElmer FTIR, UATR spectrum Two spectrometer. XPS measurements were carried out using a PHI-5000 Versa Probe III, ULVAC-PHI Inc., USA spectrometer with Al Kα radiation. XRD patterns were obtained on a Bruker D8 Advance diffractometer with Cu Kα radiation (λ = 1.5406 Å). FESEM (MIRA3 TESCAN, USA)) was used to examine morphology and coating coverage. Contact angles were measured with a DSA25 KRÜSS GmbH-Germany goniometer.

Electrochemical Measurements

Electrochemical tests were performed on a CHI162IE electrochemical workstation in a three-electrode configuration. The working electrode was bare NF or hydrogel-coated NF, the counter electrode was a Pt wire, and the reference electrode was Ag/AgCl (3M KCl). Measurements were carried out in 0.5M H_2SO_4 (acidic medium) and 1M KOH (alkaline medium). Potentials were converted to the reversible hydrogen electrode (RHE) scale. Linear sweep voltammetry (LSV) was performed at 5 mV s^{-1}. Electrochemical impedance spectroscopy (EIS) was carried out in the frequency range of 100 kHz to 0.1 Hz at an overpotential of 200 mV. Chronopotentiometry was conducted at a constant current density of -10 mA cm^{-2}. The electrochemical data obtained during the hydrogen evolution reaction

was converted to the Reversible Hydrogen Electrode scale (RHE scale) via the following equation:

$$E_{RHE} = E_{Ag/AgCl} + 0.059\ pH + E°_{Ag/AgCl} \text{ ..... (a)}$$

Bubble Force Measurements

The work by Krasowska et. al. describes the Young-Duple equation for surface tension and work of adhesion of a bubble on a substrate in a triphasic layer. It describes the surface tension of the solid-gas interphase as:

$$\gamma_{s,g} = \gamma_{l,g}(1 + cos\theta) \text{ .....(b)}$$

Where, $\gamma_{s,g}$ is the surface tension of the solid-gas interphase, $\gamma_{l,g}$ is the surface tension of the liquid-gas interface and θ is the contact angle.

The second work by Escober puts forward the total force of adhesion can be calculated by the line force acting on the bubble and the perimeter of contact for the bubble and the substrate. It can be summarized as:

$$F_{adh} = f \times \pi D \text{ .....(c)}$$

Where, Fadh is the force of adhesion, f is the line force of adhesion and D is the diameter of the bubble formed. Since, the line force acting on the bubble is the surface tension, it can be combined as:

$$F_{adh} = 2\gamma_{l,g}R(1 + cos\theta) \text{ .....(d)}$$

Where, R is the radius of the bubble.

Chitosan Viscosity Measurement:

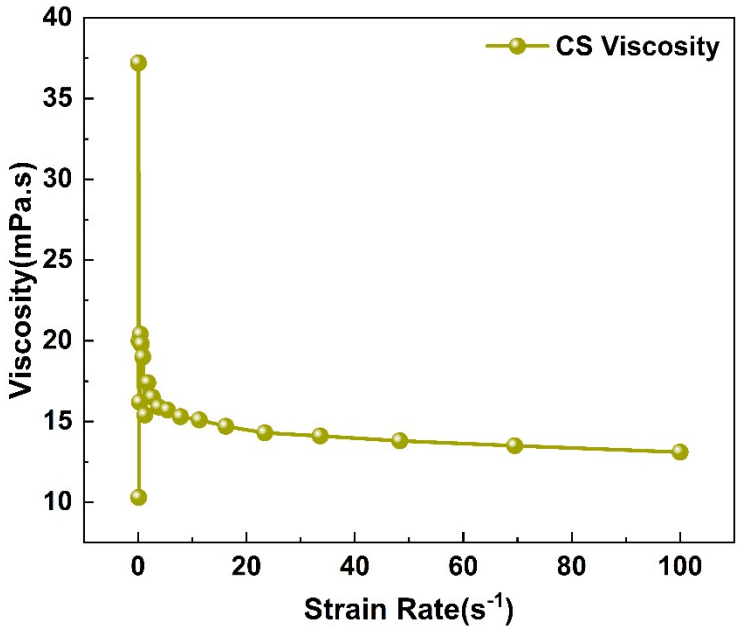

Fig. S1*. Viscosity measurement of the 2wt.% chitosan solution*

Section S2:

Bubble Diameter Measurement:

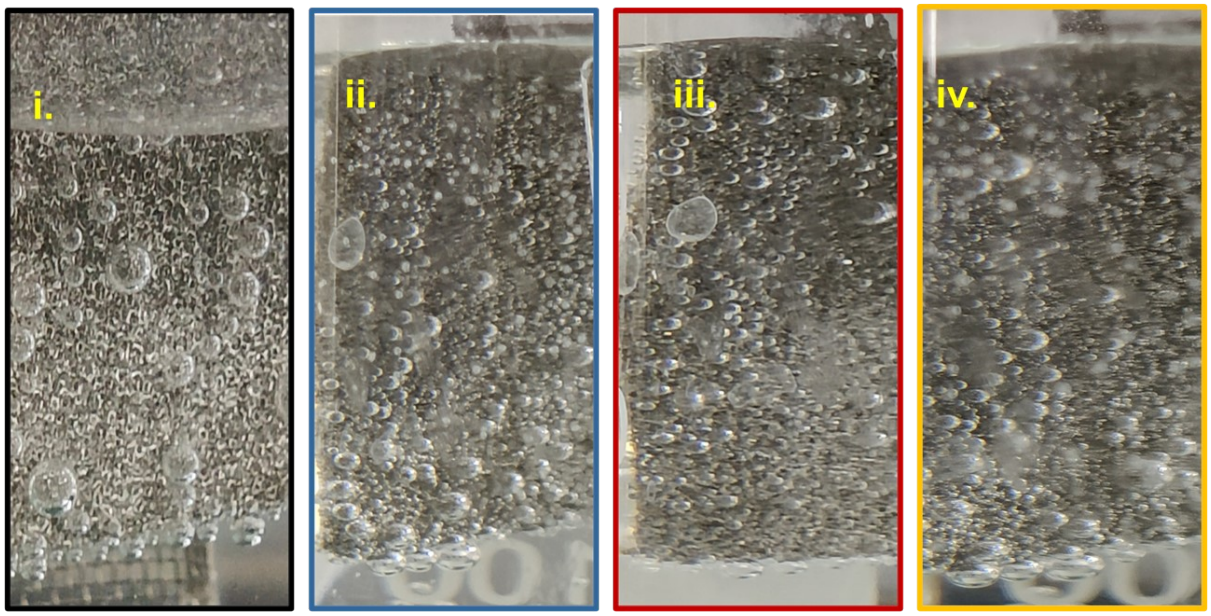

Fig. S2*: Bubble detachment from the i. Bare NF; ii. CS2.5GA; iii. CS5GA; iv. CS10GA*

Table S1: Statistical Analysis for the calculation of the bubble diameter

Normal	Normal	Normal
	mu	sigma
Bare NF	44.05628	13.30091
CS2.5GA	39.2288	14.48945
CS5GA	31.24908	8.22458
CS10GA	35.084	17.68708

Section S3:

Mechanical Strength and Swelling Behavior of the hydrogels:

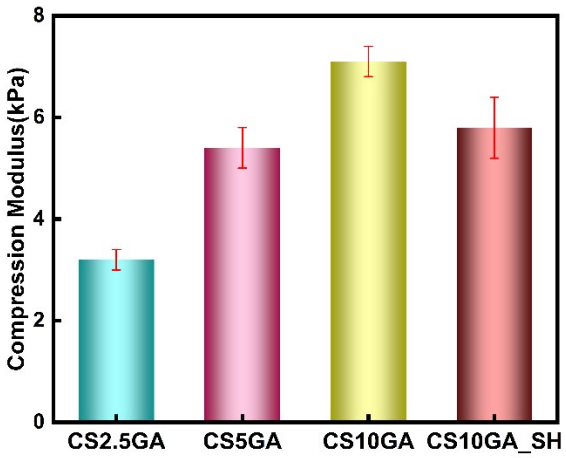

Fig. S3*. Compressive modulus of the prepared hydrogels and the self-healed CS10GA hydrogel*

The percentage of swelling of the hydrogel was calculated following the equation **(b):**

$$Swelling\ ratio\ (\%) = \frac{w_{final} - w_{initial}}{w_{initial}} \times 100\% \quad \text{..... (b)}$$

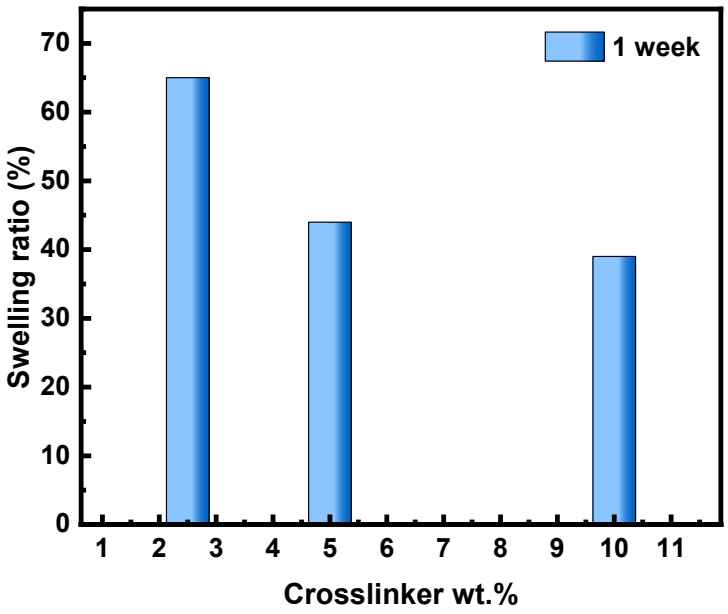

Fig. S4*. Variation of the swelling ratio of the hydrogels with crosslinker amount*

Section S4:

Analysis of the Tafel Slope Calculation

Table S2: Measurement of the Tafel from the LSV overpotentials

Equation	y = a + b*x	
Plot	\b(Bare NF)	\b(CS5GA)
Weight	No Weighting	
Intercept	0.18266 ± 0.00246	0.11558 ± 0.00145
Slope	0.30325 ± 0.00231	0.28921 ± 0.00136
Residual Sum of Squares	1.25793E-6	4.7636E-7
Pearson's r	0.99962	0.99986
R-Square (COD)	0.99925	0.99971
Adj. R-Square	0.99919	0.99969

Section S5:

C_{dl} Estimation

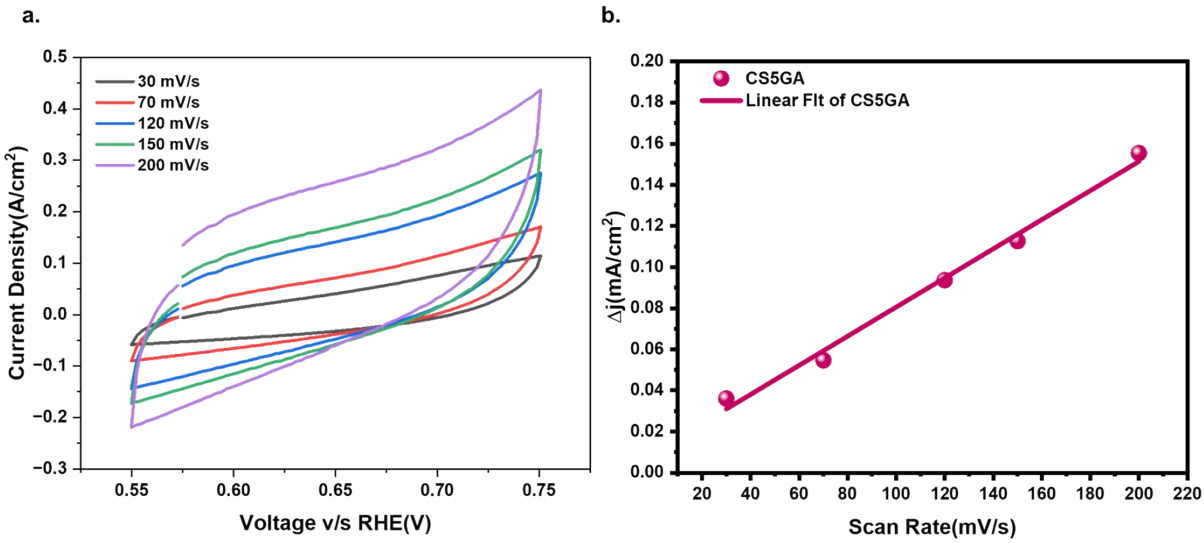

Fig. S5. *a. Cyclic voltammetry at multiple scan rate at non-Faradaic regions; b. The double-layer capacitance (C_{dl}), estimated from the linear fit of Δj/2 versus scan rate*

Section S6:

Stability Assessment:

To evaluate the chemical stability of the CS–GA hydrogel under strongly alkaline conditions, Fourier transform infrared (FTIR) spectra were recorded before and after 40 h of electrochemical HER operation in 1 M KOH (denoted as CS5GA and CS5GA_40 h, respectively). As shown in **Fig. S6**, the characteristic vibrational features of the crosslinked chitosan network are largely preserved after prolonged alkaline exposure. The broad O-H/N-H stretching band in the 3000-3500 cm^{-1} region, the C-O stretching vibrations (~1020-1080 cm^{-1}), and the amide/imine-related bands in the 1550-1650 cm^{-1} range remain clearly visible with only minor changes in intensity and bandwidth. The retention of these key bands indicates that the primary polymer backbone and the glutaraldehyde-induced crosslinked network remain chemically intact during extended HER operation in alkaline media.

A moderate increase in intensity and slight broadening of the O-H/N-H stretching region is observed after stability testing. This behavior is attributed to enhanced hydration and swelling of the hydrogel network during prolonged immersion in the alkaline electrolyte, which promotes stronger hydrogen-bonding interactions among -OH, -NH, water molecules, and OH^- ions. Such electrolyte-induced rearrangement of the hydrogen-bond network is typical for swollen hydrogel systems and reflects structural adaptation rather than chemical degradation.

Additionally, a decrease in the band around 1700-1750 cm^{-1} is noted after electrochemical operation. This band is mainly associated with residual carbonyl (C=O) vibrations related to glutaraldehyde or protonated carbonyl/imine species present in the freshly crosslinked hydrogel. Under strongly alkaline conditions, these residual aldehyde groups can undergo hydration or conversion to less IR-active species, and deprotonation of associated functionalities can further attenuate this peak. Therefore, the reduction in the ~1700-1750 cm^{-1} band is attributed to chemical equilibration of glutaraldehyde-derived carbonyl groups rather than deterioration of the chitosan backbone. Overall, the FTIR results confirm the chemical stability of the CS–GA hydrogel under prolonged alkaline HER conditions.

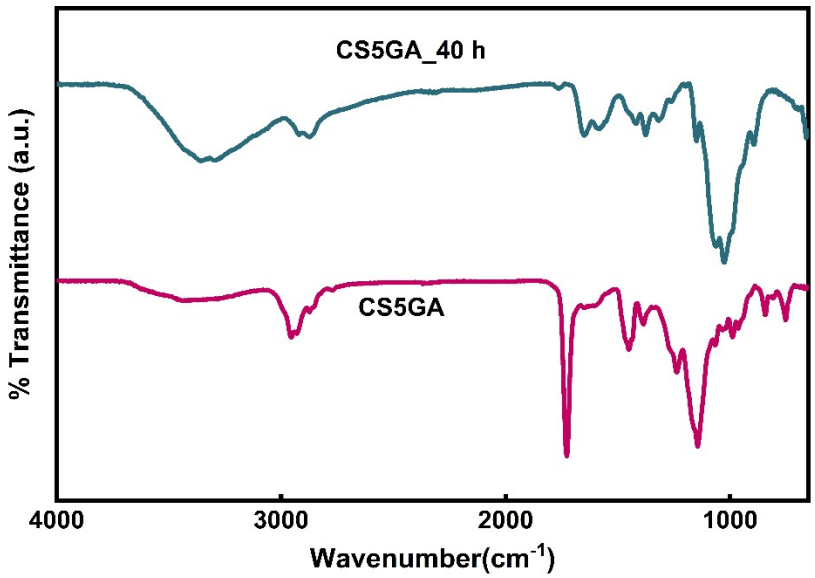

Fig. S6. *Comparison of the FTIR Spectra of the CS5GA hydrogels before and after exposure to 1M KOH for 40 h.*

Section S7:

Comparison Data:

Table S3. Comparison of the current work with the literature reported superaerophobic coatings for enhanced HER

System	Composition & Strategy	Fabrication Complexity	Bubble Management Performance	Sustainability	Key Limitation	Ref.
PEI hydrogel coating	Synthetic polyethyleneimine-based hydrogel regulating bubble detachment	Moderate (polymer synthesis + coating	Significant reduction in bubble adhesion and improved HER kinetics.	Synthetic polymer; limited bio-origin.	Relies on petrochemical polymer network	[2]
GLASS gel-like superaerophobic surface	Polyallylamine-based scalable superaerophobic gel coating	Moderate - High (spin-coating, multi-step processing	Efficient bubble release across gas-evolving reactions.	Synthetic polymer system.	Requires controlled processing and synthetic precursors.	[3]
Self-healable nanoclay-reinforced hydrogel	Synthetic polymer & inorganic nanoclay composite	High (hybrid composite preparation)	Ultralow bubble adhesion and good durability.	Partially sustainable (contains inorganic fillers)	Added fillers increase material complexity	[4]
Superaerophobic polymer hydrogels	Synthetic hydrogel coatings enabling bubble detachment	Moderate	Improved gas release and reduced overpotential	Predominantly synthetic chemistry	Limited emphasis on green/bio-derived materials	[5]
This work (CS–GA hydrogel)	Fully bio-based chitosan crosslinked with glutaraldehyde; immersion-coated on NF	Low (simple immersion + drying)	Reduction in bubble adhesion; smaller bubble size; lower Rct and overpotential	Fully bio-derived, low-cost, scalable	Does not intrinsically enhance catalytic activity (interfacial regulator only)	-

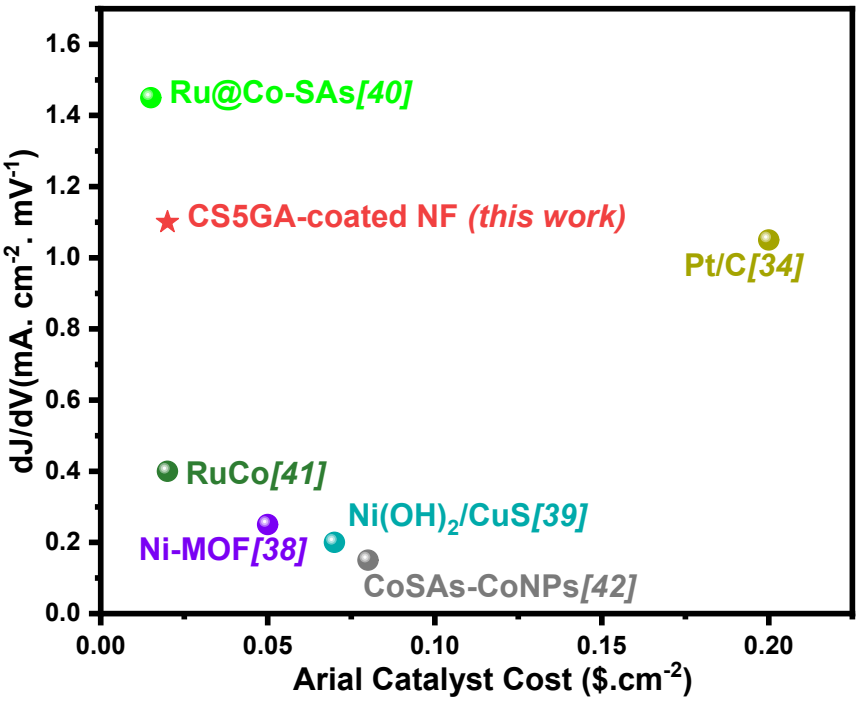

Fig S7. *Comparison of cost with performance with other state-of-the art systems*

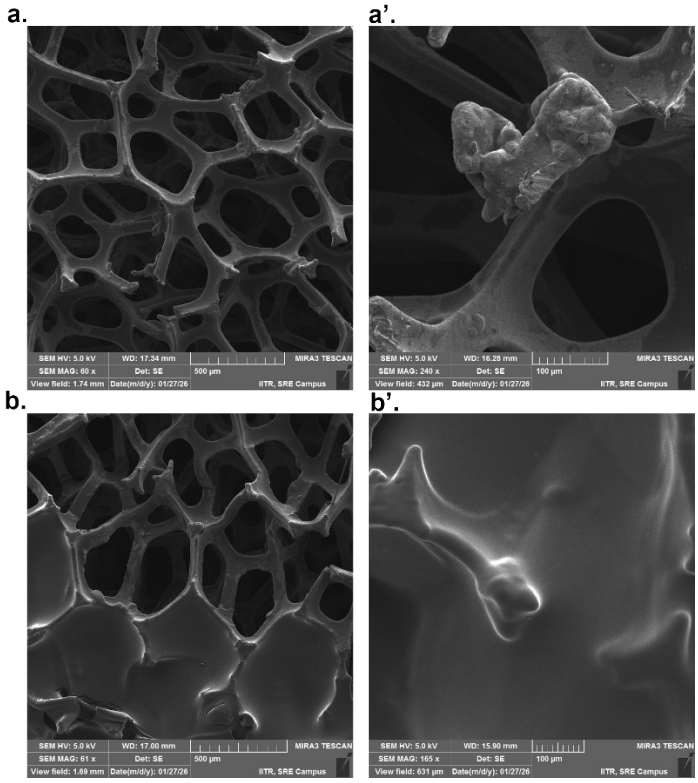

Fig S8. *Comparison of the coating characteristics of varying chitosan grades: a, a'. Chitosan grade with a 60% DD showing poor substrate coverage; b, b'. Chitosan grade with a 90% DD showing excessive coverage and blocking of the pores.*

References:

(1) Chitosan Source: Shrimp Shells Cell Culture Tested Product Code: TC242 Please Refer Disclaimer Overleaf.

(2) Bae, M.; Kang, Y.; Lee, D. W.; Jeon, D.; Ryu, J. Superaerophobic Polyethyleneimine Hydrogels for Improving Electrochemical Hydrogen Production by Promoting Bubble Detachment. *Adv. Energy Mater.* **2022**, *12* (29), 2201452. https://doi.org/10.1002/AENM.202201452.

(3) Kang, Y.; Lee, S.; Han, S.; Jeon, D.; Bae, M.; Choi, Y.; Lee, D. W.; Ryu, J.; Kang, Y.; Lee, S.; Jeon, D.; Bae, M.; Choi, Y.; Lee, D. W.; Ryu, J.; Han, S. Versatile, Stable, and Scalable Gel-Like Aerophobic Surface System (GLASS) for Hydrogen Production. *Adv. Funct. Mater.* **2024**, *34* (2), 2308827. https://doi.org/10.1002/ADFM.202308827.

(4) Sarma, H.; Mandal, S.; Borbora, A.; Das, J.; Kumar, S.; Manna, U. Self-Healable, Tolerant Superaerophobic Coating for Improving Electrochemical Hydrogen Production. *Small* **2024**, *20* (26), 2309359. https://doi.org/10.1002/SMLL.202309359.

(5) Xu, W.; Lu, Z.; Wan, P.; Kuang, Y.; Sun, X. High-Performance Water Electrolysis System with Double Nanostructured Superaerophobic Electrodes. *Small* **2016**, *12* (18), 2492–2498. https://doi.org/10.1002/SMLL.201600189.